Journal of Experimental Botany, Vol. 58, No. 14, pp. 3971–3985, 2007
doi:10.1093/jxb/erm252
This paper is available online free of all access charges (see http://jxb.oxfordjournals.org/open_access.html for further details)

Journal of Experimental Botany
www.jxb.oxfordjournals.org

RESEARCH PAPER

Expression of multiple forms of ferredoxin NADP$^+$ oxidoreductase in wheat leaves

J. O. Gummadova[1], G. J. Fletcher[1], A. Moolna[1], G. T. Hanke[2], T. Hase[2] and C. G. Bowsher[1,*]

[1] *Faculty of Life Sciences, The University of Manchester, 3. 614 Stopford Building, Oxford Road, Manchester M13 9PT, UK*

[2] *Division of Protein Chemistry, Institute for Protein Research, 3-2 Yamadaoka, Suita, Osaka 565-0879, Japan*

Received 13 August 2007; Revised 7 September 2007; Accepted 11 September 2007

Abstract

In higher plants there are two forms of ferredoxin NADP$^+$ oxidoreductase (FNR), a photosynthetic *p*FNR primarily required for the photoreduction of NADP$^+$, and a heterotrophic *h*FNR which generates reduced ferredoxin by utilizing electrons from NADPH produced during carbohydrate oxidation. The aim of this study was to investigate the presence of multiple forms of FNR in wheat leaves and the capacity of FNR isoforms to respond to changes in reductant demand through varied expression and N-terminal processing. Two forms of *pFNR* mRNA (*pFNRI* and *pFNRII*) were expressed in a similar pattern along the 12 cm developing primary wheat leaf, with the highest levels observed in plants grown continuously in the dark in the presence (*pFNRI*) or absence (*pFNRII*) of nitrate respectively. *p*FNR protein increased from the leaf base to tip. *hFNR* mRNA and protein was in the basal part of the leaf in plants grown in the presence of nitrate. FNR activity in plants grown in a light/dark cycle without nitrate was mainly due to *p*FNR, whilst *h*FNR contributed significantly in nitrate-fed plants. The potential role of distinct forms of FNR in meeting the changing metabolic capacity and reductant demands along the linear gradient of developing cells of the leaf are discussed. Furthermore, evidence for alternative N-terminal cleavage sites of *p*FNR acting as a means of discriminating between ferredoxins and the implications of this in providing a more effective flow of electrons through a particular pathway *in vivo* is considered.

Key words: Ferredoxin NADP$^+$ oxidoreductase (FNR), light, nitrogen assimilation, *Triticum aestivum*.

Introduction

Ferredoxin NADP$^+$ oxidoreductase (FNR, EC 1.18.1.2) is a ubiquitous enzyme belonging to a large family of flavoproteins found in higher plants, eukaryotic algae, photosynthetic bacteria, and animals (Arakaki *et al*., 1997). In plants, this enzyme exists in two distinct forms as a photosynthetic (*p*FNR) and as a heterotrophic (*h*FNR) form. These two isoforms are encoded by different genes, linked to different metabolic pathways and are regulated by different factors. Six genes have been identified as producing FNR-like proteins in the *Arabidopsis* genome (Wang *et al*., 2003). Of these, four have been further confirmed as producing FNR proteins, that is two *p*FNR and two *h*FNR proteins (Hanke *et al*., 2005). Two *p*FNR isoforms have been identified in *Oryza sativa* and three in *Zea mays* (maize) (Okutani *et al*., 2005; Ohyanagi *et al*., 2006). Traditionally, *p*FNR has been considered to catalyse the final step in the photosynthetic electron transport chain. Based on its association with the cytochrome b_6f complex (Zhang and Cramer, 2004) and NADP(H) dehydrogenase complex (Quiles and Cuello, 1998) and on FNR-dependent quinone reduction measurements (Bojko *et al*., 2003), *p*FNR has also been implicated to have a role in cyclic electron transport. By contrast, a role for *h*FNR has been characterized for supplying reducing power in non-photosynthetic tissue to a variety of metabolic processes including nitrate assimilation

* To whom correspondence should be addressed. E-mail: Caroline.bowsher@manchester.ac.uk
Abbreviations: Fd, ferredoxin; FdI, photosynthetic ferredoxin; FdIII, heterotrophic ferredoxin; FNR, ferredoxin NADP$^+$ oxidoreductase; *h*FNR, heterotrophic ferredoxin NADP$^+$ oxidoreductase; *p*FNR, photosynthetic ferredoxin NADP$^+$ oxidoreductase; PAGE, polyacrylamide gel electrophoresis; RT-PCR, reverse transcription-polymerase chain reaction.

(Bowsher *et al*., 1989, 1992). Sharing similar kinetic properties, *p*FNR and *h*FNR drive the same redox reaction but in opposite directions, with *p*FNR primarily reducing $NADP^+$ using electrons supplied by the photosynthetically reduced ferredoxin (Fd), and *h*FNR generating reduced Fd by accepting electrons from NADPH. *p*FNR has long been known to be regulated by light at both the transcriptional level (Neuhaus *et al*., 1993, 1997; Oelmüller *et al*., 1993; Bowler *et al*., 1994*a*, *b*) and the level of enzyme activity (Carrillo *et al*., 1981; Nikolaeva and Osipova, 1982; Pschorn *et al*., 1988*a*, *b*; Rühle *et al*., 1987). However, recent work has also shown that two *Arabidopsis p*FNR isoforms are differentially regulated by nitrate (Hanke *et al*., 2005). *h*FNR has been shown to be regulated by nitrate at both the transcriptional and enzyme levels (Bowsher *et al*., 1993*b*; Ritchie *et al*., 1994; Matsumura *et al*., 1997; Mattana *et al*., 1997; Wang *et al*., 2000, 2003; Hanke *et al*., 2005).

Despite the presence of multiple FNR isoforms and their importance in supporting a number of distinct processes which may operate simultaneously, few studies have examined whether the two differently regulated *p*FNR and *h*FNR exist in the same tissue or whether they have the potential to regulate different metabolic processes simultaneously. Both *p*FNR and *h*FNR have been detected in tomato fruit tissue (Green *et al*., 1991). In immature mung bean (*Vigna radiata* L.) immunoincubation and immunoblotting studies showed that with development and greening of young leaves *h*FNR was gradually replaced by *p*FNR (Jin *et al*., 1994; Wada *et al*., 1996). Such changes in abundance may be regulated, responding to the demand for specific metabolic processes by the plant during development and by the environment. Indeed two isoforms of *h*FNR have recently been identified in *Arabidopsis* leaves and found to be at the highest levels when grown in the presence of ammonium (Hanke *et al*., 2005). These *h*FNR isoforms or proteins have been proposed to meet the specific needs of non-photosynthetic cells in the leaf by supplying reduced Fd to support ammonium assimilation (Hanke *et al*., 2005). The 12 cm long developing primary wheat leaf has been well characterized as providing a profile of developing cells with a linear gradient of cell types. Using this developmental model of heterotrophic cells from the leaf meristem at the base of the leaf to photosynthetic cells at the tip of the leaf (Leech, 1985) provides important information as to whether, with increasing cell age, different FNR isoforms respond to changing metabolic demands during the development of photosynthesis.

This paper focuses on the identification and purification of multiple forms of FNR in wheat leaves. We first purified FNR and obtained N-terminal amino acid sequence data to investigate the FNR forms present in mature wheat leaves. Using an available wheat leaf cDNA library, FNR clones were then isolated. The effects on *p*FNR and *h*FNR transcription, protein, and activity in wheat grown in different light and nitrate environments were examined. *p*FNR with alternative N-terminal cleavage sites was overexpressed in *Escherichia coli* and, following purification, used to determine whether truncation led to potential differences in the enzymes affinity for photosynthetic and heterotrophic Fd. This complete study of the identified FNR isoforms allows us to speculate on the capacity of FNR isoforms to respond to changes in reductant demand through varied expression and N-terminal processing.

Materials and methods

Plant materials and growth conditions

For protein purification, spring wheat (*Triticum aestivum* var. Axona) was grown in John Innes No. 1 compost in a greenhouse between 15 °C and 25 °C, supplemented by sodium lights on a 16 h light (240 μmol m^{-2} s^{-1})/8 h dark cycle. All green leaves were harvested between 20 and 30 d post-anthesis and stored at –20 °C until required. To examine the developmental gradient, spring wheat, *Triticum aestivum* L. cv. Maris Huntsman, was grown in sterile Magenta vessels on 50–100 ml 0.2% (w/v) phytagel nutrient media as described by Paul and Stitt (1993). Plants were grown in a controlled environment cabinet at 20 °C in either a 16 h light (240 μmol m^{-2} s^{-1})/8 h dark cycle or continuous dark in the presence or absence of 10 mM KNO_3. Plants were harvested 4–5 h into the photoperiod after 6–7 d when leaf height had reached approximately 12 cm. Seedlings were removed from the phytagel and the roots separated from the shoots with a razor blade. Primary leaves were dissected from the seedling and then cut into six 2 cm sections, numbered section 1 at the base to section 6 at the tip. All samples were either used immediately or frozen in liquid nitrogen and stored at –80 °C until required. When using dark-grown tissue, all harvesting and extraction steps were performed in a dark room with a green safe light.

Purification of FNR from wheat leaf tissue

One kilogram of frozen wheat leaves were ground to a fine powder in a mortar and pestle in 100 g batches. All subsequent steps were carried out at 4 °C unless otherwise stated. The frozen powder was added to 2.0 l of extraction buffer [100 mM Tris-borate buffer, pH 7.7, 0.1% (v/v) β-mercaptoethanol, 1.5 % (w/v) polyvinylpolypyrrolidone, 2 mM benzamidine, 2 mM amino-*n*-caproic acid, 0.2 mM phenylmethylsulphonyl fluoride, 20 mM diethylthiocarbamate] and homogenized with a polytron into a green slurry. Following acetone precipitation (33–77%, v/v) the resulting pellet was resuspended in buffer A (10 mM TRIS-HCl, pH 7.5) and dialysed overnight against buffer A before applying to a DEAE cellulose column (2.6 cm×100 cm). The FNR was eluted with buffer A containing 100 mM NaCl and following ammonium sulphate precipitation (40–60%, w/v) the precipitate was resuspended in buffer A and dialysed against the same buffer. The sample was loaded onto a DEAE Sephacel column (1.8 cm×50 cm) and after washing with buffer A containing 100 mM NaCl, the FNR was eluted with buffer A containing 200 mM NaCl and dialysed against buffer A. The FNR sample was further purified using a ferredoxin affinity column and eluted by buffer A containing 50 mM NaCl. Following dialysis against buffer A the FNR was concentrated using a microconcentrating column (10 kDa cut-off, Amicon).

Protein extraction

Leaf soluble proteins were extracted by grinding 8–10 frozen leaf sections in 0.8 ml of extraction buffer (100 mM phosphate buffer,

pH 7.8) in a Retsch vibration mixer for 2 min. The extracts were then centrifuged at 13 000 *g* for 5 min at 4 °C. The supernatant was transferred to a fresh tube and centrifuged again. The resulting supernatant was immediately used for protein estimation, enzyme activity assays, and immunotitration. Any remaining sample was stored at –80 °C for SDS PAGE analysis.

Determination of protein concentration

Protein concentration was determined using the method of Bradford (1976), or, where limited volume was available, the method of Schaffner and Weissmann (1973).

Enzyme assays

To monitor FNR activity in the purified proteins and in tissue sections, a cytochrome *c* reduction assay system in 0.6 ml containing 50 mM TRIS-HCl, pH 7.5, 200 μM cytochrome *c*, 100 mM NaCl, and 50 μM NADPH in the presence of an NADPH regenerating system was used (Onda *et al*., 2000). The reaction was carried out at room temperature and initiated by the addition of maize FdI or FdIII at final concentrations ranging from 0–40 mM. Cytochrome *c* reduction was measured by monitoring the increase in absorbance at 550 nm. Where appropriate the kinetic constants K_m and V_{max}, were calculated with non-linear regression analysis using the Solver function in Microsoft Excel 97 (Microsoft, Redmond, WA).

To monitor FNR activity eluted from columns, diaphorase activity was measured in an NADPH-dependent reduction of nitroblue tetrazolium (Swegle and Mattoo, 1996), using a microtitre based assay. 100 mM TRIS-HCl, pH 7.5, 1 mM nitro-blue tetrazolium, 2 mM NADPH, and 1 μl of extract were combined in a 100 μl final assay volume and the optical density change monitored at 540 nm.

SDS polyacrylamide gel electrophoresis (PAGE)

The SDS-PAGE of proteins was performed on 12.5% acrylamide gels according to Hames and Rickwood (1990). The gels were stained for protein with Coomassie Brilliant Blue (0.1% w/v Coomassie Brilliant Blue, 25% v/v methanol, 8% v/v acetic acid, 67% v/v water) or silver (Wray *et al*., 1981).

Preparation of protein samples for N-terminal-amino-acid determination

SDS-PAGE of FNR, blotting and amino acid sequence determination was performed as described previously (Bowsher *et al*., 1993*a*).

Isoelectric point determination

The isoelectric point of mature proteins was calculated using the available cDNA sequence information and the predictive program at EXPASY (http://www.expasy.org/tools/pi_tool.html). To determine the isoelectric points experimentally 0.1–1 μg overexpressed *p*FNR proteins were loaded onto 18 cm polyacrylamide gel strips with an immobilized linear gradient of pH 4–7 (Immobiline DryStrip, Amersham) and focused in a Protean isoelecric focusing cell (Bio-Rad) according to the manufacturers instructions. The second dimension was run with 15% SDS-PAGE using the Protean II xi vertical gel electrophoresis system (Bio-Rad). The location of the *p*FNR spots was visualized using either blue-silver Coomassie G-250 total protein staining (Candiano *et al*., 2004) or by immunoblotting with the PEP*p*FNR antibody. All gels and blots were scanned using Quantity One gel imaging software and the GS-710 calibrated imaging densitometer (Bio-Rad). The positions of each of the *p*FNR spots were measured according to the linear pH gradient and were consistent in four independent replicates.

Antibody production

Synthetic peptides were designed to produce PEP*p*FNR antiserum based on information obtained from the Swissprot and Trembl databases of protein sequences (http://www.expasy.ch). In the absence of a complete amino acid sequence for wheat, FNR peptides were selected based on the *p*FNR sequence of rice, a related species (Aoki *et al*., 1994). *h*FNR and *p*FNR sequences were aligned using the Clustal W multiple sequence alignment program. Disparate regions of between 12–15 amino acids were selected from the rice *p*FNR amino acid sequence (Aoki *et al*., 1994) on the basis of low amino acid identity with rice root *h*FNR (Aoki and Ida, 1994). Regions were identified with less than 34% identity to *h*FNR and then mapped onto a three-dimensional model of *p*FNR based on the Karplus crystallographic structure of spinach *p*FNR (Karplus, 1991). Two surface-orientated peptides, peptide I, ISKKH-DEGVVTNK, and peptide IV, ADGVDKNGKPHKL, located in continuous domains of the Karplus crystallographic structure were used to synthesize multiple antigen peptides. One mg of each peptide was dissolved in 1 ml of 25 mM TRIS-HCl, pH 8.0, divided into three aliquots and each aliquot mixed with an equal volume of Freunds adjuvant prior to injecting a sheep at monthly intervals (Diagnostics Scotland). Three individual bleeds were taken from the sheep and dilutions of the final bleed used for all subsequent experiments without further purification.

Immunoblotting

For immunoblotting, following separation by SDS-PAGE proteins were electroblotted to a nitrocellulose or PVDF membrane and incubated with antibody raised against *p*FNR or *h*FNR. The antigen–antibody complex was visualized by reaction with alkaline phosphatase or horseradish peroxidase conjugated secondary antibody. Equal loading of protein samples was confirmed by total protein staining of the blots with Ponceau S solution prior to incubation with the specific antibody.

Immunotitration using pea h*FNR antisera*

Pea *h*FNR antiserum (Bowsher *et al*., 1993*a*) was diluted with 100 mM TRIS-HCl pH 7.6 to 50% (v/v). One volume of leaf section extract was mixed with 1 vol. of the diluted antiserum and incubated with gentle shaking (150 rpm) at 4 °C for 90 min. The antibody–antigen complex was removed from the solution by centrifugation at 13 000 *g* for 30 min at 4 °C. The supernatant was carefully transferred to a fresh tube and assayed for cytochrome *c* reduction activity. Control serum had no effect on the FNR activity. Immunoblots of samples confirmed that immunodepletion of samples had occurred.

RNA preparation

RNA was prepared using LiCl precipitation based on the method of Knight and Gray (1994). mRNA was isolated from total RNA based on Poly (A) Quick mRNA isolation kit (Stratagene).

RNA hybridization

For RNA blot hybridization 10–20 μg of the isolated total RNA from each section was denatured with formaldehyde and subjected to electrophoresis and blotted onto a Hybond N^+ membrane as described previously (Fonseca *et al*., 1997). The probe used for the hybridization was either a 1 400 bp *Pisum sativum p*FNR cDNA (Newman and Gray, 1988), a 252 bp partial clone for wheat *h*FNR, or a 1 000 bp *Triticum aestivum* rRNA cDNA clone. In all cases, DNA probes were radiolabelled with [α-^{32}P]-dCTP using a random priming kit (Stratagene), prehybridized, hybridized, and exposed to film as described previously (Fonseca *et al*., 1997). Autoradiograms

were scanned and relative amounts of mRNAs determined as described previously (Fonseca *et al*., 1997).

RNA loading control and relative mRNA levels

All the RNA blots were incubated with specific probes under the same conditions and subsequently exposed to film for the same period of time. To equalize the total amount of RNA run on the gels for loading error and to allow comparisons of gene expression along the wheat leaf under different environmental conditions to be analysed statistically, all the membranes were reprobed with a 1 000 bp wheat 18S rRNA cDNA as a housekeeping gene. Again, as with the specific probes, all the membranes were tested under the same conditions. The reprobed membranes were exposed for identical periods of time. The detected signals were scanned and quantitated by the densitometry analysis program AIDA200. The releative mRNA level of the gene was estimated as a ratio of its band density to that of the respective rRNA band. At least three replicates were performed for each treatment.

Library screening

A high-titre complementary DNA library was initially prepared with mRNA isolated from wheat (*Triticum aestivum* cv. Maris Huntsman) leaves grown for 14 d in the presence of 10 mM nitrate, using the ZAP Express cDNA synthesis kit and ZAP Express cDNA Gigapack III gold cloning kit and according to the manufacturer's instructions (Stratagene Ltd). More than 300 000 phage were initially screened using a 1 400 bp pea *p*FNR cDNA (Newman and Gray, 1988), a 1 300 bp pea *h*FNR cDNA (Bowsher and Knight, 1996), or a 1 200 bp *Oryza sativa h*FNR cDNA (Aoki and Ida, 1994) fragment as a probe, radiolabelled with [α-^{32}P]dCTP (3 000 Ci mmol^{-1}) using Prime-it II Random Primer Labelling kit (Stratagene) as described previously (Davis *et al*., 2003). Following overnight hybridization at 50–65 °C and depending on the stringency required, filters were washed sequentially using 2× SSC and 0.1% SDS, 1× SSC and 0.1% SDS, and 0.1× SSC and 0.1% SDS at 50–65 °C. Positive clones were confirmed by subsequent secondary and tertiary screens.

Reverse transcription-polymerase chain reaction

Total RNA (0.05–0.5 μg) from wheat roots or basal leaf 2 cm sections was used to manufacture cDNA using the In-promII reverse transcription kit (Promega) according to the manufacturer's instructions. Degenerate primers for polymerase chain reaction (PCR) were as follows: hFNR 5′-AAG/AGAA/GGAT/CCCIA-GIAAG/AAA-3' and 5′-GCIACICCIAG/AG/AAAIAG/TCCA-3′. Each PCR was performed with 1/10, 1/100, and 1/1 000 dilutions of cDNA. PCR was hot started at 94 °C and carried out for 30 cycles of 94 °C for 1 min, 50 °C for 1 min, and 72 °C for 2 min. Following agarose gel electrophoresis, products were visualized by 0.0001% (w/v) ethidium bromide staining.

PCR amplification of the 5′ ends of p*FNRI and* p*FNRII*

Primers for PCR amplification of the 5' end of *p*FNRI cDNA coding region were as follows: 5′-GCCACCGCCGCCTCCACC-3' and 5′-GCACTTGCCCACGCTGACA-3′. Primers for PCR amplification of 5' end of *p*FNRII cDNA coding region were as follows: 5′-ATGGCCGCCCAGCTGACA-3' and 5′-GAGATCTTCACC-GGCTTG-3′. PCR was hot started at 94 °C and carried out for 30 cycles of 94 °C for 45 s, 55 °C for 45 s, and 72 °C for 2 min, followed by a final extension at 72 °C for 7 min.

Sequence alignment

The FNR sequences were aligned using the Kalign multiple sequence alignment algorithm at http://msa.cgb.ki.se/cgi-bin/msa.cgi (Lassmann and Sonnhammer, 2005). GenBank accession numbers used were as follows: maize leaf (BAA88236, BAA88237), maize root (AAB40034), rice leaf (NP_001056570, NP_001045608), rice root (BAA02248), arabidopsis leaf (CAB52472, AAF79911), and arabidopsis root (CAB81081, AAM65564).

Preparation of overexpressed FNRs

The *p*FNRI and *p*FNRII cDNA clones were used as a template to generate a PCR product corresponding to the FNR gene. Two alternative *p*FNRI and *p*FNRII forms were generated based on the available N-terminal sequence data. Primers were designed to incorporate the *Nco*1 site for the sense primer and a *Bam*HI site for the antisense primer. In the case of the latter this was located downstream of the stop codon for either the *p*FNRI or *p*FNRII gene. Initially, the PCR product was cloned into the pQE60 vector between the *Nco*I and *Bam*HI sites. The truncated forms of *p*FNRI and *p*FNRII were made by mutagenesis of these clones. The full and truncated FNRs were overexpressed with either TG1 or JM109 *E. coli* strains transformed with the prepared vector and purified using a ferredoxin affinity column (Onda *et al*., 2000).

Statistical analysis

Statistical tests of Analysis of Variance (ANOVA) were performed using SPSS statistical software version 11.0 (SPSS Inc). Analysis of variance was performed in order to determine whether there were differences in the means between groups for mRNA levels or enzyme activity values in different conditions/treatments. Univariate ANOVA applied the principles of testing for population mean differences to situations involving more than two comparison groups. The analysis requesting multiple comparison (post hoc) tests were performed to see specifically which population groups differed. Multivariate ANOVA applied the principles of testing for differences in population means to situations involving more than one factor.

Results

Purification of FNR from wheat leaves

FNR-like proteins were purified over 350-fold from wheat leaves using a mixture of acetone precipitation, ion-exchange chromatography, ammonium sulphate precipitation, and ferredoxin affinity chromatography (data not shown). The purified FNR had a final specific activity of 105 μmol cytochrome *c* reduced min^{-1} mg^{-1} protein. After SDS-PAGE and Coomassie Brilliant Blue staining (Fig. 1) or silver staining (data not shown) four protein bands (I, II, III, and IV) were observed. The molecular weights of these four polypeptides were estimated by SDS-PAGE to be 35, 34, 32, and 31 kDa. When challenged with available antibody raised against *Pisum sativum p*FNR or *h*FNR, only bands I, II, and III were detected by the *p*FNR antibody (Fig. 1). N-terminal amino acid sequence data were obtained for the individually excised protein bands (I–IV). Band III was found to be composed of two distinct N-terminal sequences, IIIa and IIIb. All five sequences were compared for similarities to rice *p*FNR and *h*FNR (Fig. 2). Proteins I, II, IIIa, and IIIb all showed good sequence identity between the sequence

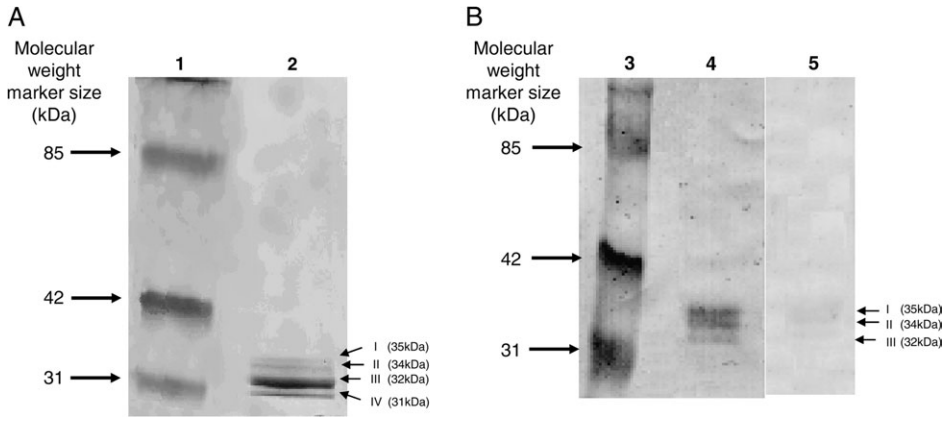

Fig. 1. SDS-PAGE of the purified ferredoxin NADP⁺ oxidoreductase sample eluted from the ferredoxin affinity column. Proteins were separated by SDS-PAGE and (A) stained with Coomassie Brilliant Blue R or (B) immunoblotted to nitrocellulose membrane and challenged with *p*FNR (lane 4) or *h*FNR (lane 5) antibody. Lanes 1, 3: molecular weight markers; lanes 2, 4, 5: 7.7 μg of protein eluted from the ferredoxin affinity column. The bands detected from the ferredoxin affinity column were designated I=35 kDa, II=34 kDa, III=32 kDa, and IV=31 kDa.

pFNR		E	K	I	S	K	K	H	D	E	G	V	V	T	N	K	Y
Band I		K	K	V	S	K	K	Q	E	E							
Band II					*	K	K	Q	E	E	G	V	V	T			
Band IIIa				I	S	K	K	Q	D	E	G	V	V	K	N		
Band IIIb						K	K	Q	D	E	G	V	V	T	N	T	Y
hFNR		A	V	K	P	L	D	L	E	S	A	N	E	P	P	L	N
Band IV					(YYPPEEYYGGGLLN)												

Fig. 2. Comparison of N-terminal sequences obtained for the wheat proteins eluted from the ferredoxin affinity column. Polypeptides were separated on a 12.5% SDS–polyacrylamide gel and sequenced by Edman degradation. An asterisk indicates that there was uncertainty in the identity of an amino acid residue. For comparative purposes the *p*FNR and *h*FNR sequences from rice (Aoki *et al*., 1994; Aoki and Ida, 1994) are shown. Band I, II, III, and IV correspond to the numbers on the SDS-PAGE gel shown in Fig. 1.

data obtained with that previously published for rice *p*FNR. Band IV showed no identity with either *p*FNR or *h*FNR.

Isolation of wheat leaf FNR clones

Following the final screen of the wheat leaf library, eight cDNA clones of varying length (1 350–3 050 bp) were sequenced. Based on their nucleotide similarity, the clones represented two main groups *p*FNRI and *p*FNRII. The nucleotide sequences corresponding to the coding regions of both clones and their deduced protein sequences were submitted to the GenBank database and given the accession numbers AJ457979 (CAD30025) and AJ457980 (CAD30024), respectively. *p*FNRI is composed of 1 047 bp, whereas *p*FNRII consists of 1 092 bp (Fig. 3). *p*FNRI and *p*FNRII share 80% overall similarity at the amino acid level. However, the N-terminal 45–55 amino acids, corresponding to the transit peptide region, share less than 25% sequence identity. Using the available N-terminal sequence data, alternative cleavage points of the chloroplast transit peptide for *p*FNRI and *p*FNRII could be identified in each cDNA clone. The mature protein regions of both *p*FNRI and *p*FNRII showed good sequence identity to other leaf FNRs (Fig. 3). The deduced amino acid sequence of wheat *p*FNRI had 84% identical residues with maize *p*FNRI (Onda *et al*., 2000), whilst the wheat *p*FNRII had 76% sequence identity to maize *p*FNRI (Onda *et al*., 2000) and 88% sequence identity to maize *p*FNRII. These data, in conjunction with the N-terminal cDNA data, were used to predict the isoelectric point of the alternative mature proteins purified from wheat leaves (Table 1). *p*FNRII is notably more acidic than *p*FNRI. The alternative N-terminal cleavage sites of *p*FNRI, $pFNRI_{KKVS}$, and $pFNRI_{SKKQ}$ appear to affect the predicted pI with the shorter $pFNRI_{SKKQ}$ having a markedly more acidic isoelectric point. By contrast, the alternative N-terminal cleavage sites for *p*FNRII, $pFNRII_{ISKK}$, and $pFNRII_{KKQD}$ appear to have little effect on the predicted isoelectric point of the proteins.

When the wheat leaf library was screened using available rice (Aoki *et al*., 1994) or pea (Bowsher and Knight, 1996) root *h*FNR cDNA fragments as probes, no corresponding *h*FNR cDNA clones were identified. In an alternative RT-PCR approach, multiple alignment of available plant *h*FNR sequences was used to identify consensus sequences which could be used to design degenerate primers. A 252 bp product was amplified using total RNA from either nitrate-fed wheat roots or the leaf base. Alignment with known *h*FNR cDNAs confirmed that the isolated PCR product belonged to the *h*FNR class of proteins (Fig. 4). The wheat *h*FNR fragment shared 90–94% identity with rice (Aoki and Ida, 1994) and maize *h*FNR (Ritchie *et al*., 1994) and 57% with both the wheat *p*FNRI and *p*FNRII reported here.

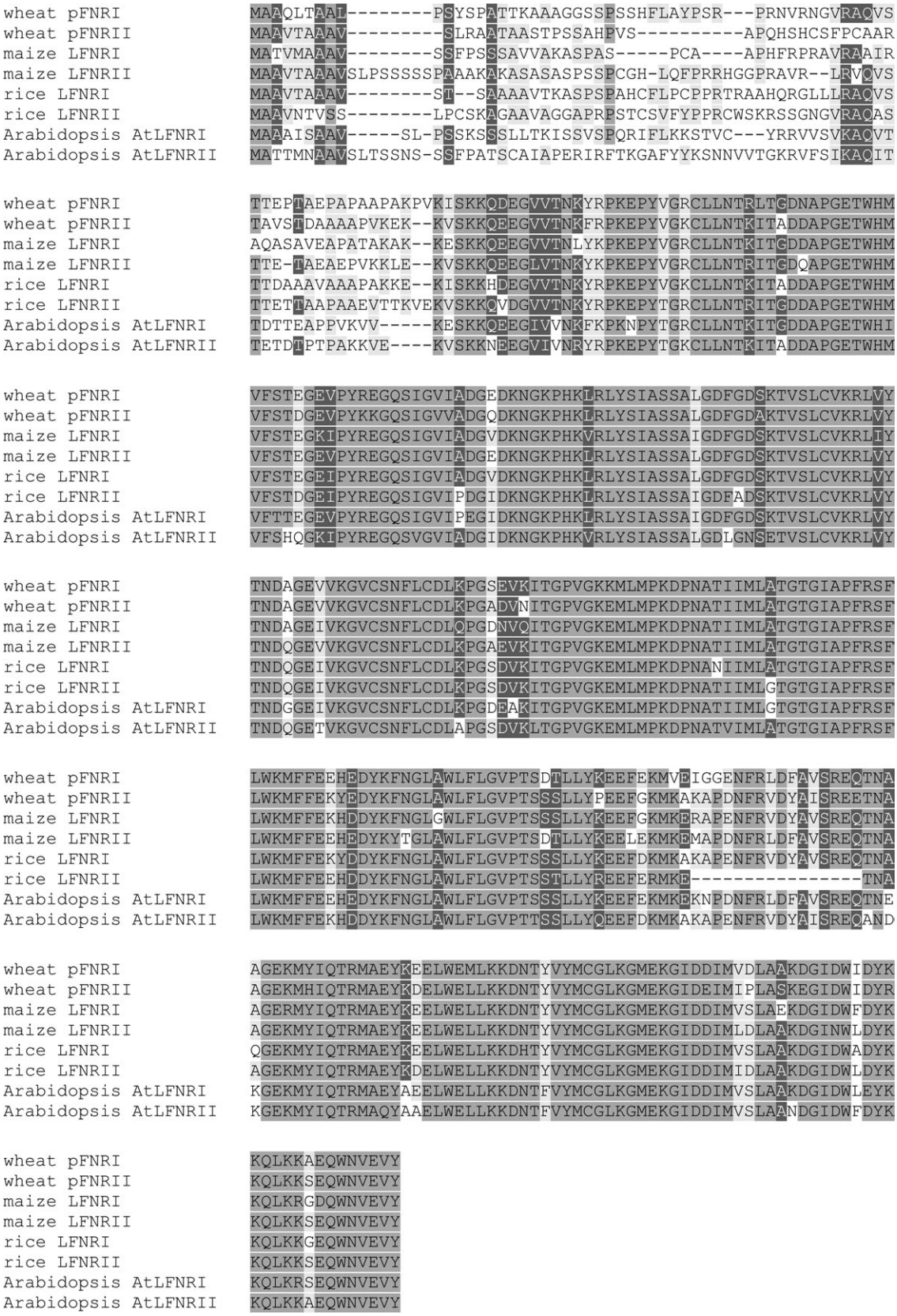

Fig. 3. ClustalW multiple alignment of the deduced amino acid sequences of wheat *p*FNRI, *p*FNRII with some known *p*FNR amino acid sequences. Sequence alignments were carried out as described in the Materials and methods. The alignment was performed using the deduced amino acid sequences of maize (Okutani *et al*., 2005; Onda *et al*., 2000), rice (Ohyanagi *et al*., 2006), and *Arabidopsis* (Hanke *et al*., 2005). Similar residues are shown in dark grey, strongly similar residues in grey, weakly similar in light grey.

Table 1. *Summary of the effect of N-terminal truncation on the isoelectric point (pI) of* p*FNRI and* p*FNRII*

*p*FNR proteins with alternative N-terminal cleavage points were overexpressed in *E. coli* and purified using a ferredoxin affinity column. Following isoelectric focusing the actual pI was determined for each protein and compared with the predicted pI (see Materials and methods for further details).

*p*FNR isoform	N-terminal sequence	pI (Predicted)	pI (Actual)	Molecular weight (kDa)
*p*FNRI	KKVSKKQE	8.12	6.73	33.52
*p*FNRI	SKKQE	6.82	6.40	33.17
*p*FNRII	ISKKQD	5.50	5.42	33.49
*p*FNRII	KKQD	5.50	5.44	33.29

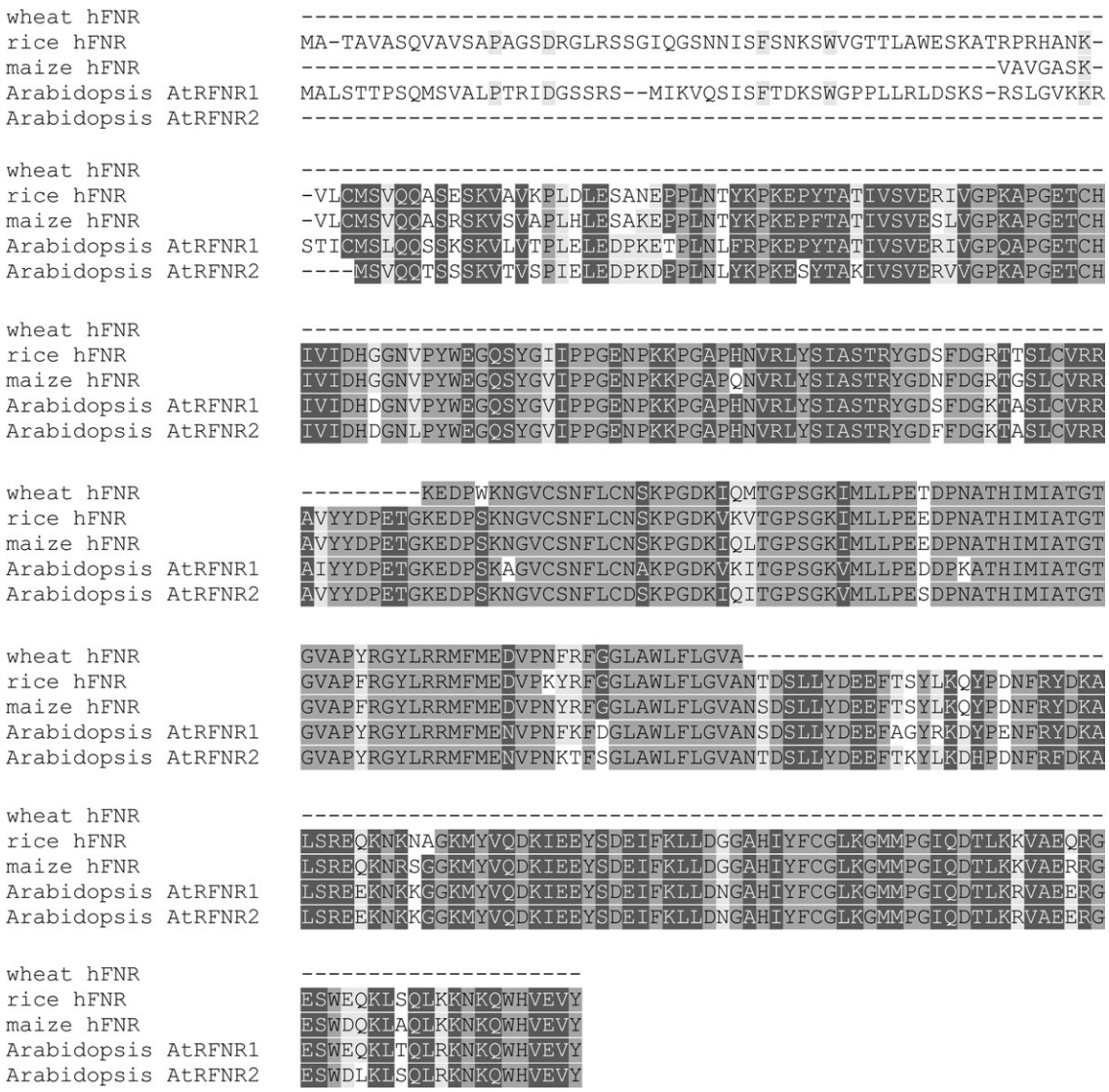

Fig. 4. ClustalW multiple alignment of the deduced amino acid sequence of the wheat 252 bp hFNR cDNA fragment with other plant hFNRs. The alignment was performed using the deduced amino acid sequences of rice (Aoki and Ida, 1994), maize (Ritchie *et al*., 1995), and *Arabidopsis* (Hanke *et al*., 2005). Similar residues are shown in dark grey, strongly similar residues in grey, weakly similar in light grey.

Comparison of overexpressed wheat proteins with alternative N-terminal cleavage points

To investigate further whether there was any functional significance related to alternative N-terminal start sites, $p\text{FNRI}_{\text{KKVS}}$, $p\text{FNRI}_{\text{SKKQ}}$, $p\text{FNRII}_{\text{ISKK}}$, and $p\text{FNRII}_{\text{KKQD}}$ were overexpressed in *E. coli* and purified using a ferredoxin affinity column as described previously (Onda *et al*., 2000). The *p*FNR proteins purified from recombinant bacterial cells showed absorption spectra typical of flavin containing enzymes (data not shown). The

isoelectric point of each overexpressed protein was determined by isoelectric focusing and compared with the predicted values (Table 1). As expected, the *p*FNRII proteins had more acidic pIs than those of the *p*FNRI proteins. Furthermore, N-terminal truncation of *p*FNRI did lead to a more acidic pI, although the shift was not as marked as that predicted (Table 1). The kinetic properties of purified *p*FNR proteins were determined using either photosynthetic type ferredoxin (FdI) or heterotrophic ferredoxin (FdIII) from maize as described for maize FNR (Onda *et al*., 2000; Table 2). Irrespective of ferredoxin type, recombinant *p*FNRII proteins had a 2-fold higher activity than *p*FNRI isoforms, but considerably lower affinity. Differences in the N-terminal of recombinant *p*FNRI, did not greatly affect K_m and V_{max} values with either FdI or FdIII, although the shorter $pFNRI_{SKKQ}$ had consistently lower activity than the longer $pFNRI_{KKVS}$. By contrast, the longer version of *p*FNRII, $pFNRII_{ISKK}$ discriminated between photosynthetic and heterotrophic ferredoxins (having an approximate 3-fold lower K_m for the heterotrophic FdIII) while the shorter $pFNRII_{KKQD}$ did not. The removal of two N-terminal residues from *p*FNRII appeared to increase the affinity for FdIII to approximately the same value as FdI.

pFNR *and* hFNR *expression in different light and nitrogen conditions*

FNR is involved not just in photosynthesis but also in providing reductant for a range of ferredoxin-dependent reactions. Previous experiments using microarray studies and the transfer of plants between different nitrogen regimes have confirmed isoform specific involvement of FNR in *Arabidopsis* (Wang *et al*., 2000; Hanke *et al*., 2005) and maize (Okutani *et al*., 2005). To monitor changes in *pFNR* or *hFNR* relative steady-state transcript abundance along the primary wheat leaf, plants were grown continuously in the presence or absence of 10 mM nitrate and in either a 16/8 h light/dark cycle or continuous dark (Fig. 5). RNA was extracted from 2 cm sections along the 12 cm leaf from the base to the tip. To distinguish between *pFNRI* and *pFNRII* genes in northern blotting analysis, the areas of least identity in the *p*FNRI and *p*FNRII cDNAs, corresponding to the region coding for the transit peptide and the N-termini, were chosen for subsequent amplification of a probe. The 252 bp partial clone for wheat *h*FNR was used to study the gene expression of the *hFNR* isoform. The specificity of each probe was confirmed even under conditions of low stringency. The expression of each clone significantly varied between the base, middle, and tip of the wheat leaf.

Both *pFNRI* and *pFNRII* were expressed in a similar pattern along the wheat leaf. However, the highest levels of *pFNRI* and *pFNRII* mRNA were observed in the dark in the presence or absence of nitrate respectively (Fig. 5). *hFNR* mRNA expression was highest in the base and showed a marked decline along the wheat leaf under all growth conditions. The addition of nitrate in the light led to a significant up-regulation of *hFNR* mRNA levels. This effect of nitrate on gene expression was only significant in the light, although the effect of light alone on *hFNR* mRNA levels did not appear to be important. It was also shown that, in the dark, there was a highly significant dependence of *hFNR* mRNA production on the position along the leaf developmental gradient.

Table 2. *Summary of the effect of N-terminal truncation on the kinetic properties of* p*FNRI and* p*FNRII in a NADPH-dependent cytochrome* c *reduction assay*

*p*FNR proteins with alternative N-terminal cleavage points were overexpressed in *E. coli* and purified using a ferredoxin affinity column (see Materials and methods for further details). K_m and V_{max} were calculated following double reciprocal plots. The data represents the mean of at least three independent determinations.

Overexpressed *p*FNR isoform	FdI		FdIII	
	K_m	V_{max}	K_m	V_{max}
$pFNRI_{KKVS}$	1.80±0.36	52.76±2.40	1.93±0.12	46.73±1.21
$pFNRI_{SKKQ}$	2.47±0.15	44.23±1.17	2.98±0.27	38.83±1.27
$pFNRII_{ISKK}$	28.60±4.61	119.63±8.57	11.13±0.76	117.87±3.21
$pFNRII_{KKQD}$	8.35±0.58	110.60±1.51	9.28±0.45	125.90±8.67

Changes in the p*FNR and* h*FNR protein levels in variable light and nitrogen conditions*

Specific antibodies, PEP*p*FNR and pea *h*FNR, were used to distinguish between *p*FNR and *h*FNR (Fig. 6). The amount of *p*FNR protein detected by the PEP*p*FNR antibody gradually increased from the leaf base to tip in all sets of growth conditions (Fig. 6). By contrast, *h*FNR protein was detected in the basal part of the leaf under all growth conditions (Fig. 6). In leaves grown in the light and nitrate set of conditions, *h*FNR was detected along the entire wheat leaf (Fig. 6).

Changes in p*FNR and* h*FNR enzyme activity in variable light and nitrogen conditions*

The contribution of each FNR isoform to measured enzyme activity in the wheat leaf was determined by using an immunoprecipitation approach (Fig. 7). Leaf extracts from different sections along the wheat leaf were incubated in the presence or absence of a constant amount of *h*FNR antibody and the total FNR activity measured in a cytochrome *c* reduction assay. The total FNR activity measured in each section in the absence of antibody was taken as 100% (comprising both *p*FNR and *h*FNR). In the presence of *h*FNR antibody, *h*FNR activity was precipitated and therefore the activity measured in the assay represented that of *p*FNR only. Figure 7 shows the proportion of *p*FNR and *h*FNR activity as a percentage of the total FNR activity in the crude extract. In the light and nitrate treatment, *p*FNR and *h*FNR activity represents 4%

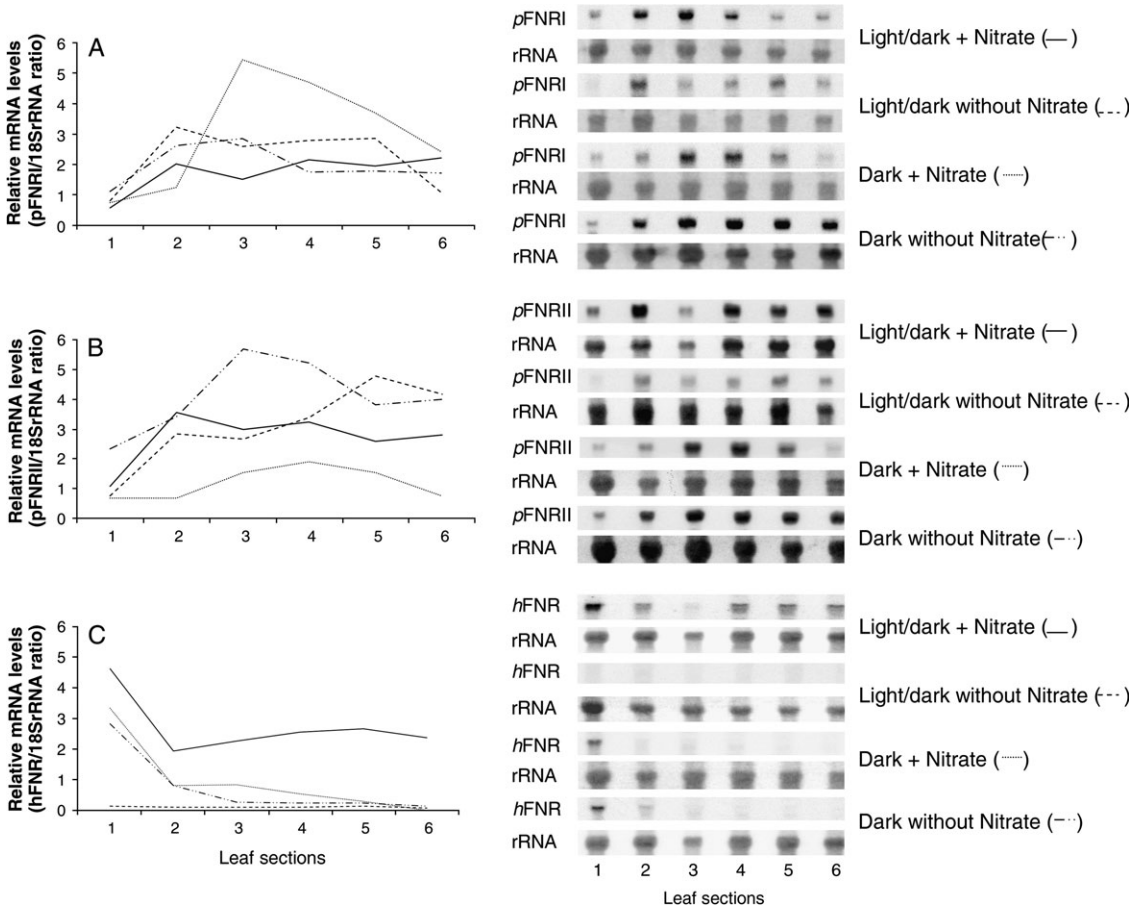

Fig. 5. Expression of (A) *p*FNRI, (B) *p*FNRII, and (C) *h*FNR along the length of a 12 cm primary wheat leaf grown for 7 d as described in the Materials and methods under a light/dark cycle in the presence of nitrate (—); light/dark cycle in the absence of nitrate (– – –); continuous dark in the presence of nitrate (....); continuous dark in the absence of nitrate (-··-··-). The 12 cm long primary wheat leaves were harvested, cut into six sections from the base (section 1) to the tip (section 6) and total RNA was isolated and 20 μg subjected to northern analysis. Each blot was probed with the indicated FNR cDNA and then reprobed with the internal standard 18S rRNA. The films were exposed for the same duration of time in the case of each FNR being studied and compared with the internal standard (18S rRNA). The graphs presented represent the northern blot analysis where the data are expressed as the ratio of *p*FNRI; *p*FNRII, and *h*FNR to 18S rRNA after quantitation by densitometry. Experiments were repeated at least three times and representative blots for each treatment are shown.

and 96%, respectively, of the total FNR activity at the base (section 1) of the leaf. In the light without nitrate, *p*FNR and *h*FNR activity represented 27% and 73%, respectively, of the total FNR activity at the leaf base (section 1). The proportion of *p*FNR activity in the sections towards the leaf tip of plants grown in light without nitrate increased to reach 100% in sections 5 and 6. By contrast, there was no measurable enzyme activity detected in leaf tissue in the dark in either the presence or absence of nitrate.

Discussion

The aim of this study was to investigate the presence of multiple forms of FNR in wheat leaves and the capacity of FNR isoenzymes to respond to changes in reductant demand through varied expression and N-terminal processing. The 12 cm primary wheat leaf provides an ideal model system to investigate changes in response to development. To our knowledge, this is the first report of such a study on FNR. The purification of FNR from wheat leaf tissue led to the identification of four polypeptides. Based on N-terminal sequencing these proteins corresponded to two alternative N-termini versions of each *p*FNRI and *p*FNRII. Subsequent screening of a wheat leaf cDNA library confirmed the presence of *p*FNRI and *p*FNRII. Furthermore, the use of an RT-PCR approach led to the identification of a *h*FNR clone in wheat leaves.

Changes in p*FNR levels along the developmental gradient of a wheat leaf*

12 cm long primary wheat leaves represent a linear developmental gradient of increasing cell age, with immature dividing heterotrophic cells at the base and mature photosynthetic cells at the tip. There is a gradient of cellular and plastid development along the wheat leaf

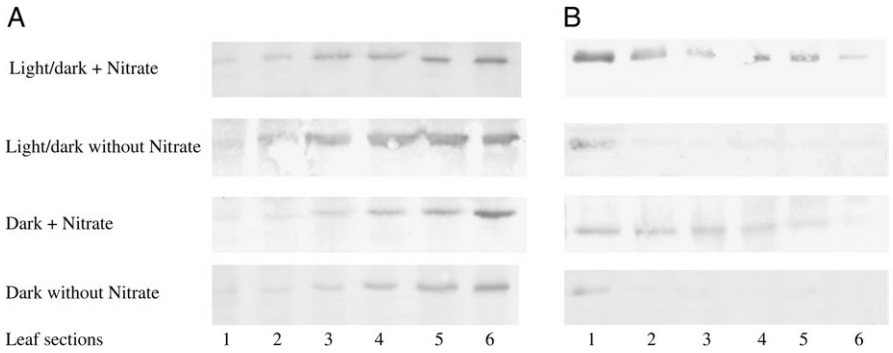

Fig. 6. Changes in (A) *p*FNR and (B) *h*FNR protein levels along the length of a 12 cm primary wheat leaf grown for 7 d under variable light and nitrogen conditions as described in the Materials and methods. The 12 cm long primary wheat leaves were harvested, cut into six sections from the base (section 1) to the tip (section 6) and 50 μg of protein extract separated by SDS-gel electrophoresis, transferred onto a Protran membrane and treated with either (A) PEP*p*FNR or (B) pea *h*FNR primary antibody. Experiments were repeated at least three times and representative blots for each treatment are shown.

(Dean and Leach, 1982*a*, *b*). By preparing sections along the leaf it is possible to investigate homogeneous populations of leaf cells and plastids of different developmental ages within the same leaves. Using this system allowed changes to be studied in FNR expression, protein, and enzyme activity with development, nitrate supply and light regime. The pattern of *pFNR* mRNA expression, protein and enzyme activity was similar in all experimental conditions, with lowest levels at the leaf base. Conversely, *hFNR* mRNA, protein, and enzyme activity tended to be highest at the leaf base and declined towards the tip of the leaf (Fig. 8).

Much of the available literature has identified the short-term response of *p*FNR at the transcriptional level via light-responsive *cis* elements and at the level of the enzyme (Neuhaus *et al*., 1993, 1997; Oelmüller *et al*., 1993; Bolle *et al*., 1994*a*, *b*; Bowler and Chua, 1996; Lübberstedt *et al*., 1994*a*, *b*). By contrast our study examined the impact of more long-term exposure to environmental factors, confirming that high levels of *pFNRI* and *pFNRII* mRNA and protein were present in either set of light conditions. Interestingly, the highest mRNA levels for both *pFNRI* and *pFNRII* were observed in the dark suggesting light does not play a significant long-term role in triggering and maintaining high levels of transcription of the *pFNR* encoding genes. In the dark-grown plants the highest expression was in the mid-leaf region and this may reflect an anatomical or developmental cue overridden and masked by light. In plants grown in the absence of light but in the presence of nitrate, there was a marked differential response with *pFNRI* expression increased and *pFNRII* expression decreased. Although the level of *p*FNR protein increased towards the wheat leaf tip under all conditions, no other more subtle differences in the protein levels in response to nitrate or dark growth conditions were identified. This probably reflects the inability of the antibody used (PEP*p*FNR) to distinguish between the different *p*FNR forms. This is further confirmed in experiments with *Arabidopsis* where the steady-state transcript levels of *AtLFNRII* were highest and *AtLFNR1* transcripts were less abundant in plants grown in a light/dark cycle in the presence of high nitrate (Hanke *et al*., 2005). These data in wheat, together with that observed in *Arabidopsis*, support the suggestion that the two *pFNR* genes have distinct and separate functional roles. Recently, studies of *Arabidopsis* FNR knockout lines showed that *AtLFNRI* and *AtLFNRII* could not fully replace each others activity. The homozygous knockout line *AtLFNRI* had reduced capacity for C fixation and a decreased biomass accumulation (Lintala *et al*., 2007).

The physiological importance of N-terminal variants of p*FNR*

Since the original work of Keirns and Wang (1972) the presence of multiple forms of FNR have been confirmed by several laboratories (e.g. Karplus *et al*., 1984). The enzyme from *Spinacia oleracea* has been extensively studied and there have been discrepancies concerning the number of forms and their physical and chemical properties. In spinach, two closely migrating protein bands on SDS-polyacrylamide gels were suggested to arise from degradation of the larger form at the N-terminus (Shin *et al*., 1990). Although the alternative N-terminal cleavage sites identified in the work reported here for wheat may have arisen as a result of proteolytic degradation, this is unlikely since proteolytic protectants were included in all buffers during the initial stages of the purification. Furthermore where protein samples were prepared directly from fresh tissue of frozen extracts (stored at –20 °C or –80 °C) or directly from isolated chloroplasts, a similar pattern of multiple FNR proteins was identified using SDS-PAGE (data not shown). Recently, an NMR comparison of the effects on the N-terminal and C-terminal end of the FNR polypeptide chain of substrate interactions indicated that there are profound

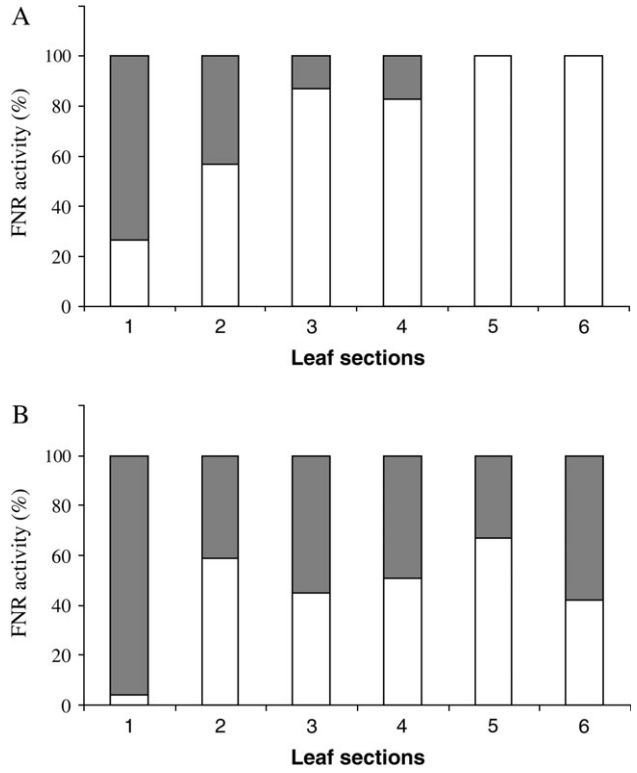

Fig. 7. Changes in *p*FNR and *h*FNR enzyme activity along the length of a 12 cm primary wheat leaf grown for 7 d under (A) light without nitrate and (B) light with nitrate as described in the Materials and methods. The 12 cm long primary wheat leaves were harvested, cut into six sections from the base (section 1) to the tip (section 6) and total FNR activity was measured using a cytochrome *c* dependent assay. *h*FNR activity was removed by incubating the leaf extract with pea *h*FNR antiserum (black bars) and any remaining FNR activity was measured using a cytochrome *c* dependent assay and assumed to represent *p*FNR activity (white bars). Each value represents the mean of three replicates. 100% represents the total FNR activity determined in the leaf extract for each section in the absence of immunotitration with the *h*FNR antibody.

effects on the N-terminus of the FNR (Maeda *et al*., 2005). In studies by Gadda *et al*. (1990) N-terminal truncated forms of FNR had full diaphorase capacity, but lost the ability to catalyse the ferredoxin-dependent reaction. As such, the alternative cleavage sites identified for both *p*FNRI and *p*FNRII in this study may have important implications for the functionality of FNR with, for example, its interaction with ferredoxin. Based on both the predicted and actual isoelectric points, *p*FNRI and *p*FNRII may be assigned as basic and acidic, respectively. This is in agreement with work published on maize (Okutani *et al*., 2005) and *Arabidopsis* (Hanke *et al*., 2005; Lintala *et al*., 2007) isoforms. Interestingly, although the alternative N-terminal forms of *p*FNRII had very similar isoelectric points, the alternative cleavage site for *p*FNRI, $pFNRI_{KKVS}$, and $pFNRI_{SKKQ}$, resulted in a marked change in the predicted isoelectric point. This latter difference was further confirmed by isoelectric focusing of the overexpressed *p*FNRI, although the impact of the N-terminal truncation on the overall pI was not as marked as the predicted value. Overexpression of these alternative forms of *p*FNR allowed us to investigate whether this N-terminal truncation has any potential effect on the kinetic properties of either *p*FNRI or *p*FNRII. Of all the overexpressed *p*FNR forms assayed, only the longer form of *p*FNRII, $pFNRII_{ISKK}$, showed a clear discrimination between the different forms of Fd with a notably higher K_m for the photosynthetic FdI when compared to the heterotrophic FdIII. The two amino acid N-terminal truncation to $pFNR_{KKQD}$ eliminated this discrimination, bringing the K_m for FdI to a level equivalent to that for non-photosynthetic FdIII. In previous work, maize FNRI was also unable to discriminate between these photosynthetic and heterotrophic forms of Fd (Onda *et al*., 2000).

N-terminal truncation might be a form of post-transcriptional regulation operating alone or in combination with other regulatory mechanisms. For example, a suggested role for protein phosphorylation has been proposed. However, although possible sites have been identified *in silico*, these have still not been confirmed *in vivo (*Hodges and Miginiac-Maslow, 1993; Lintala *et al*., 2007). Multiple putative subforms of FNR exhibiting different enzymatic activities may reflect a specific metabolic role, for example, cyclic or non-cyclic electron flow. Truncated N-terminal forms of *p*FNR with differential abilities to discriminate between different ferredoxins may enable the more effective flow of electrons through particular pathways.

The differences in the N-termini of the FNR may also result in different modes of association with thylakoids. This assumption was originally proposed by Wada *et al*. (1996) after detecting free-state *h*FNR and partly thylakoid-bound *p*FNR in the same tissues. It was further supported when more than one leaf FNR were characterized for *Arabidopsis* (Hanke *et al*., 2005) and maize (Okutani *et al*., 2005). Multiple *p*FNR subforms could represent free and thylakoid-bound populations within the chloroplast also differing in function. In previous work by Hanke *et al*. (2005), studying *p*FNR, the more acidic *At*FNRI was the most abundant form in the thylakoids and the less acidic *At*FNRII was mostly present in the stroma. This might suggest the less acidic wheat $pFNRI_{KKVS}$ is in the stroma and the more acidic truncated $pFNRI_{SKKQ}$ is in the thylakoids. Although the N-terminal truncation of *p*FNRII has no apparent impact on the isoelectric point, the observed effect of this truncation on the K_m and V_{max} of *p*FNRII and its ability to discriminate between different Fd isoproteins needs to be investigated further to understand the possible functional implications and whether this is of importance *in vivo*. This supports the idea that the plant system is similar to cyanobacteria where distribution of FNR between thylakoids and the phycobilosome fraction provides a mechanism for sharing electrons between linear and cyclic electron flow (Van Thor *et al*., 1998, 2000). Interestingly, recent work using *Arabidopsis*

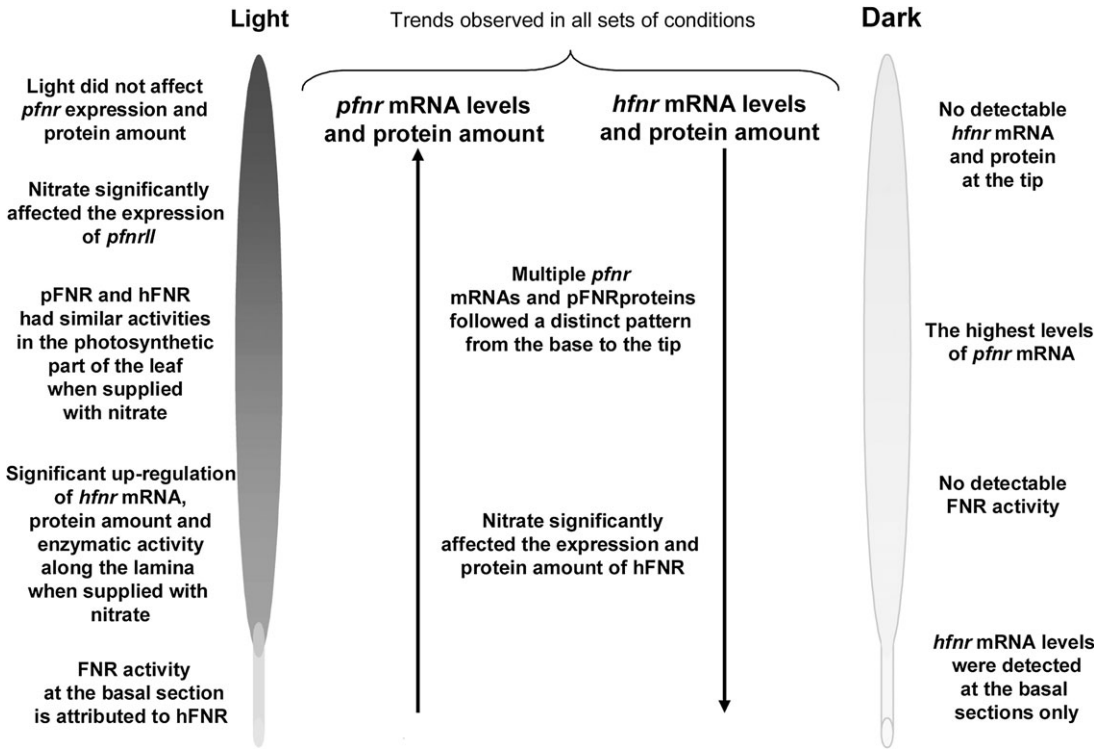

Fig. 8. Summary of the *p*FNR and *h*FNR regulation along the length of a 12 cm primary wheat leaf grown for 7 d under variable light and nitrogen conditions.

mutants has suggested that the absence of the acidic *AtLFNRI* prevented association of the basic *AtLFNRII* with the thylakoid membrane (Lintala *et al*., 2007). Dimer formation may, depending on environmental cues, be a way to regulate the distribution of electrons between the cyclic and linear electron transfer pathway (Lintala *et al*., 2007).

Although it is not known whether the specific isoforms of FNR identified in this study are catalytically more likely to support specific metabolic processes, we can propose a model where, for example, depending on the photosynthetic status of the cell, multiple *p*FNR forms might be distributed between the cyclic and non-cyclic electron flow (Shahak *et al*., 1981). In cyclic electron flow, electrons from PSI are returned to the quinone pool via ferredoxin (and an unknown Fd:quinone reductase) or NADPH (and the Ndh complex), generating ATP with no net reduction of NADPH (Takabayashi *et al*., 2005). A close association of FNR with the chloroplastic Ndh complex was described in potato and barley (Guedeney *et al*.,1996; Quiles and Cuello, 1998; Funk *et al*., 1999). Teicher and Scheller (1998) demonstrated that Ndh in barley thylakoids was activated by light and accounted for 40% of ferredoxin-dependent cyclic electron-transport rates. Depending on the location of bound *p*FNR, it could create a NADPH-rich mini-environment, stimulating cyclic electron transfer through the Ndh complex. The over-reduced ferredoxin, resulting from an increased NADPH/NADP ratio, can enhance the diversion of the electrons into the cytochrome *b*/*f* complex, thus triggering the cyclic flow (Kimata-Ariga *et al*., 2000). This has important implications for plant metabolism providing firstly, an additional supply of ATP and, secondly, a defensive mechanism against photo-oxidative damage and salt stress (Canaani, 1990; Heber and Walker, 1992). The presence of multiple FNR forms which are regulated independently and can interact differently along the wheat leaf provides added flexibility to allow the plant to adapt to a changing metabolic environment.

h*FNR in the developing wheat leaf*

hFNR mRNA was undetectable in leaf tissue grown in the light in the absence of nitrate, although there was protein and enzyme activity detectable in the basal section. The highest levels of *hFNR* mRNA, protein, and enzyme activity were demonstrated in the leaf base section and decreased towards the leaf tip in the presence of nitrate. Since the basal cells of the cereal leaf are non-photosynthetic (Thompson *et al*., 1998), one can envisage a role for *h*FNR in these cells in providing reductant non-photosynthetically via the oxidative pentose phosphate pathway for a range of metabolic processes (Bowsher *et al*., 2007). In agreement with previously published results on the short-term nitrate induction of *hFNR*-encoding genes in roots (Ritchie *et al*., 1994; Mattana *et al*., 1997), the continuous presence of nitrate has a significant effect on *h*FNR expression, protein, and enzyme activity in leaf tissue. A

transient induction of *h*FNR in *Arabidopsis* (Wang *et al*., 2003) and maize (Sakakibara, 2003) shoots transferred to nitrate has been reported. However, more recently, studies on *Arabidopsis* plants growing on high nitrate reported that only low steady-state levels of *h*FNR levels were detected in leaf tissue (Hanke *et al*., 2005). Interestingly when *Arabidopsis* plants were grown continuously in the presence of ammonium, the levels of *h*FNR increased, again confirming the potential importance of this isoform in green tissue during nitrogen metabolism (Hanke *et al*., 2005). Such a discrepancy in *h*FNR induction between wheat and *Arabidopsis* leaves may reflect a difference between photosynthetic and non-photosynthetic cells distribution in monocotyledonous and dicotyledonous plants.

A role for FNR in linking carbon and nitrogen metabolism

The use of the *h*FNR antibody in immunoprecipitation experiments meant the contribution of *p*FNR and *h*FNR to the total FNR enzyme activity measured could be distinguished. The apparent switch from one protein form to another occurs between the base and middle or between the middle and apical parts of the leaf. The presence of multiple *p*FNR subforms and *h*FNR in wheat leaf tissue appears to be dependent on the presence or absence of light and/or nitrate. Different isoforms of FNR may have similar functions within the cell, but operate in either distinct cell types or developmental periods. However, it is also possible that different isoforms may have distinct non-overlapping functions within the same cell. The heterogeneity of cell types along a wheat leaf and the apparent influence of the developmental gradient along the wheat leaf on the FNR forms present, most likely reflects the involvement of the different isoforms and indeed subforms specializing in specific types of electron transfer in response to changing metabolic demands along the leaf.

In leaves in the light, ferredoxin transfers photon-generated reducing power to nitrite reductase, to glutamate synthase, and to $NADP^+$ via FNR. Therefore, enzymatic activities fundamental to carbohydrate synthesis from CO_2 and the reduction of nitrite to ammonia and its incorporation into glutamate, all depend on reduced ferredoxin. Interestingly, the supply of reduced ferredoxin via *h*FNR seems to be a limiting factor when optimal nitrite reductase and glutamate synthase activity are operating in non-photosynthetic root plastids (Bowsher *et al*., 2007). The contribution of *p*FNR and *h*FNR in meeting the needs for reductant supply to support nitrogen assimilation in the leaves under non-photosynthetic conditions is not known. However, leaves contain a large proportion of cells with functions other than photosynthesis and of the total cell population in 12 cm illuminated wheat leaves, only 45% in the leaf base and 55% in the leaf tip are chloroplast containing mesophyll cells (Dean and Leach, 1982*a*, *b*). Furthermore while chloroplasts are located in mesophyll cells, plastids are also found in, for example, vascular tissue, which can contribute as much as 5% of the total leaf cells, and in epidermal cells, that contribute another 10–20% (Bowsher and Tobin, 2001). Such a distribution of *p*FNR and *h*FNR between mesophyll and heterotrophic cells, respectively, and the changing metabolic needs of different cells may account for the variation seen in gene expression, protein amount, and enzyme activity values observed in this current study. *h*FNR activity in a heterotrophic direction and therefore its presence along the wheat leaf most likely reflects an auxillary role under conditions of high ferredoxin demand in the leaf, such as high nitrate growth conditions.

Using the model of the 12 cm primary wheat leaf has provided us with a system to examine how multiple FNR isoforms change in response to development and different light and nitrate environments along the leaf. The switch from *h*FNR at the base of the leaf to multiple *p*FNR forms reflects a change in heterotrophic metabolism in the leaf meristem, to increasing photosynthetic capacity as leaf cells move towards the leaf tip. Although the two forms of *p*FNR show a similar pattern of expression along the leaf, clearly different forms respond in a different manner to nitrate and the dark. Furthermore the forms may also associate differently based on the metabolic demands. This study has identified the presence of multiple forms of FNR in wheat leaves with varied expression and N-terminal processing. This provides the leaf with the potential flexibility to respond to changes in reductant demand in a number of ways. For example, depending on the photosynthetic status of the cell, the presence of multiple *p*FNR forms may reflect their distribution between the cyclic and non-cyclic electron flow. This situation may be further regulated by the role of isoform-dependent N-terminal truncations in functionality. Clearly N-terminal truncation leads to some discrimination between Fd isoforms *in vitro*. We are currently investigating the physiological significance of this *in vivo*.

Acknowledgements

This work was supported in part by funding from The Royal Society, and the BBSRC (Grant JPA 886). GJF and AM were in receipt of BBSRC studentships. JOG was funded by grants from the Open Society Institute (New York, USA) and the Central European University (Budapest, Hungary). Wheat was grown by Mr Thurston Heaton at the Firs Experimental Grounds, The University of Manchester. pFNR antibody was kindly supplied by Professor J Gray (Cambridge).

References

Arakaki AK, Ceccarelli EA, Carrillo N. 1997. Plant-type ferredoxin-$NADP^+$ reductases: a basal structural framework and a multiplicity of functions. *FASEB Journal* **11,** 133–140.

Aoki H, Doyama N, Ida S. 1994. Sequence of a cDNA-encoding rice (*Oryza sativa* L.) leaf ferredoxin NADP(+) reductase. *Plant Physiology* **104,** 1473–1474.

Aoki H, Ida S. 1994. Nucleotide sequence of a rice root cDNA and its induction by nitrate. *Biochimica et Biophysica Acta* **1183,** 553–556.

Bojko M, Kruk J, Wieckowski S. 2003. Plastoquinones are effectively reduced by ferredoxin:$NADP^+$ oxidoreductase in the presence of sodium cholate miscelles: significance for cyclic electron transport and chlororespiration. *Phytochemistry* **64,** 1055–1060.

Bolle C, Sopory S, Lübberstedt T, Herrmann RG, Oelmüller R. 1994*a*. Segments encoding 5' untranslated leaders of genes for thylakoid proteins contain *cis*-elements essential for transcription. *The Plant Journal* **6,** 513–523.

Bolle C, Sopory S, Lübberstedt T, Klösgen RB, Herrmann RG, Oelmüller R. 1994*b*. The role of plastids in the expression of nuclear genes for thylakoid proteins studied with chimeric β-glucuronidase gene fusions. *Plant Physiology* **105,** 1355–1364.

Bowler C, Chua NH. 1996. Emerging themes of plant signal transduction. *The Plant Cell* **6,** 1529–1541.

Bowler C, Neuhaus G, Yamagata H, Chua NH. 1994*a*. Cyclic GMP and calcium mediate phytochrome phototransduction. *Cell* **77,** 73–81.

Bowler C, Yamagata H, Neuhaus G, Chua NH. 1994*b*. Phytochrome signal transduction pathways are regulated by reciprocal control mechanisms. *Genes and Development* **8,** 2188–2202.

Bowsher CG, Boulton EL, Rose J, Nayagam S, Emes MJ. 1992. Reductant for glutamate synthase is generated by the oxidative pentose phosphate pathway. *The Plant Journal* **2,** 893–898.

Bowsher CG, Dunbar B, Emes MJ. 1993*a*. The purification and properties of ferredoxin-$NADP^+$ oxidoreductase from roots of *Pisum sativum* L. *Protein Purification and Expression* **4,** 512–518.

Bowsher CG, Hucklesby DP, Emes MJ. 1989. Nitrite reduction and carbohydrate metabolism in plastids purified from roots of *Pisum sativum*. L. *Planta* **177,** 359–366.

Bowsher CG, Hucklesby DP, Emes MJ. 1993*b*. Induction of ferredoxin-$NADP^+$ oxidoreductase and ferredoxin synthesis in pea root plastids during nitrate assimilation. *The Plant Journal* **3,** 463–467.

Bowsher CG, Knight JS. 1996. The isolation of a pea root ferredoxin $NADP^+$ oxidoreductase (FNR) cDNA. *Plant Physiology* **112,** 861.

Bowsher CG, Lacey AE, Hanke GT, Clarkson DT, Saker LR, Stulen I, Emes MJ. 2007. The effect of Glc6P uptake and its subsequent oxidation within pea root plastids on nitrite reduction and glutamate synthesis. *Journal of Experimental Biology* **58,** 1109–1118.

Bowsher CG, Tobin AK. 2001. Compartmentation of metabolism within mitochondria and plastids. *Journal of Experimental Botany* **52,** 513–527.

Bradford MM. 1976. A rapid and sensitive method for the quantitation of microgram quantities of protein utilizing the principle of protein–dye binding. *Analytical Biochemistry* **72,** 248–254.

Canaani O. 1990. The role of cyclic electron flow around photosystem I and excitation energy distribution between the photosystems upon acclimation to high ionic strength in *Dunaliella*. *Phytochemistry and Photobiology* **52,** 591–599.

Candiano G, Bruschi M, Musante L, Santucci L, Ghiggeri GM, Carnemolla B, Orecchia P, Zardi L, Righetti PG. 2004. Blue silver: a very sensitive colloidal Coomasie G-250 staining for proteome analysis. *Electrophoresis* **25,** 1327–1333.

Carrillo N, Lucero HA, Vallejos RH. 1981. Light modulation of chloroplast membrane-bound ferredoxin-NADP-oxidoreductase. *Journal of Biological Chemistry* **256,** 1058–1059.

Davis EJ, Tetlow IJ, Bowsher CG, Emes MJ. 2003. Molecular and biochemical characterization of cytosolic phosphoglucomutase in wheat endosperm (*Triticum aestivum* L. cv. Axona). *Journal of Experimental Botany* **54,** 1351–1360.

Dean C, Leech RM. 1982*a*. Genome expression during normal leaf development. 1. Cellular and chloroplast numbers and DNA, RNA and protein levels in tissue of different ages within a seven-day-old wheat leaf. *Plant Physiology* **69,** 904–910.

Dean C, Leech RM. 1982*b*. Genome expression during normal leaf development. 2. Direct correlation between ribulose bisphosphate carboxylase content and nuclear ploidy in a polyploid wheat series. *Plant Physiology* **70,** 1605–1608.

Fonseca F, Bowsher CG, Stulen I. 1997. Impact of elevated CO_2 on nitrate reductase transcription and activity in leaves and roots of *Plantago major*. *Physiologia Plantarum* **100,** 940–948.

Funk E, Schafer E, Steinmüller S. 1999. Characterization of the complex I: homologous NAD(P)H plastoquinone-oxidorereductase (NDH-complex) of maize chloroplasts. *Journal of Plant Physiology* **154,** 16–23.

Gadda G, Aliverti A, Ronchi S, Zanetti G. 1990. Structure–function relationships in spinach ferredoxin–$NADP^+$ reductase as studied by limited proteolysis. *Journal of Biological Chemistry* **266,** 11955–11959.

Green LS, Yee BC, Buchanan BB, Kamide K, Sanada Y, Wada K. 1991. Ferredoxin and ferredoxin NADP reductase from photosynthetic and non-photosynthetic tissues of tomato. *Plant Physiology* **96,** 1207–1213.

Guedeney G, Corneille S, Cuine S, Peltier G. 1996. Evidence for an association of ndh B, ndh J gene products and ferredoxin-NADP-reductase as components of a chloroplastic NAD(P)H dehydrogenase complex. *FEBS Letters* **378,** 277–280.

Hames BD, Rickwood D. 1990. *Gel electrophoresis of proteins: a practical approach*, 2nd edn. Oxford: IRL Press.

Hanke GT, Okutani S, Satomi Y, Takao T, Suzuki A, Hase T. 2005. Multiple iso-proteins of FNR in *Arabidopsis*: evidence for different contributions to chloroplast function and nitrogen assimilation. *Plant, Cell and Environment* **28,** 1146–1157.

Heber U, Walker DA. 1992. Concerning a dual function of coupled cyclic electron transport in leaves. *Plant Physiology* **100,** 1621–1626.

Hodges M, Miginiac-Maslow M. 1993. The *in vitro* effects of ATP and protein phosphorylation on the activity of ferredoxin:$NADP^+$ oxidoreductase from spinach chloroplasts. *Plant Science* **90,** 21–29.

Jin T, Morigasaki S, Wada K. 1994. Purification and characterization of two ferredoxin $NADP^+$ oxidoreductase from the first foliage leaf of the mung bean (*Vigna radiata*) seedlings. *Plant Physiology* **106,** 697–702.

Karplus PA. 1991. Atomic structure of ferredoxin $NADP^+$ reductase; prototype for a structurally novel flavoenzyme family. *Science* **252,** 368–377.

Karplus PA, Walsh KA, Herriot JR. 1984. Amino acid sequence of spinach ferredoxin:$NADP^+$ oxidoreductase. *Biochemistry* **23,** 6576–6583.

Keirns JJ, Wang JH. 1972. Studies of nicotinamide adenine dinucleotide phosphate reductase of spinach chloroplasts. *Journal of Biological Chemistry* **247,** 7374–7382.

Kimata-Ariga Y, Matsumura T, Kada S, Fujimoto H, Fujita Y, Endo T, Mano J, Sato F, Hase T. 2000. Differential electron flow around photosystem I by two C_4-photosynthetic-cell-specific ferredoxins. *EMBO Journal* **19,** 5041–5050.

Knight JS, Gray JC. 1994. Expression of genes encoding the tobacco chloroplast phosphate translocator is not light regulated and is repressed by sucrose. *Molecular and General Genetics* **242,** 585–594.

Lassman T, Sonnhammer ELL. 2005. Kalign: an accurate and fast multiple sequence alignment algorithm. *BMC Bioinformatics* **6,** 298.

Leech RM. 1985. The synthesis of cellular components in leaves. In: Baker NR, Davies WJ, Ong CK, eds. *Control of leaf growth*. Society for Experimental Biology Seminar Series, No 27, Cambridge: Cambridge University Press, 93–114.

Lintala L, Allahverdiyeva1 Y, Kidron H, Piippo M, Battchikova1 N, Suorsa1 M, Rintamäki E, Salminen TA,

Aro E-M, Mulo P. 2007. Structural and functional characterization of ferredoxin-NADP⁺-oxidoreductase using knock-out mutants of Arabidopsis. *The Plant Journal* **49,** 1041–1052.

Lübberstedt T, Bolle CEH, Sopory S, Flieger K, Herrmann RG, Oelmüller R. 1994*a*. Promoters from genes for plastid proteins possess regions with different sensitivities towards red and blue light. *Plant Physiology* **104,** 997–1006.

Lübberstedt T, Oelmüller R, Wanner G, Herrmann RG. 1994*b*. Interacting *cis*-elements in the plastocyanin promoter from spinach ensure regulated high-level expression. *Molecular and General Genetics* **242,** 602–613.

Maeda M, Lee YH, Ikegami T, Tamura K, Hoshimo M, Yamazaki T, Nakayama M, Hase T, Goto Y. 2005. Identification of the N- and C- terminal substrate binding segments of ferredoxin-NADP⁺reductase by NMR. *Biochemistry* **44,** 10644–10653.

Matsumura T, Sakakibara H, Nakano R, Kimata Y, Sugiyama T, Hase T. 1997. A nitrate-inducible ferredoxin in maize roots. *Plant Physiology* **114,** 653–660.

Mattana M, Ida S, Reggiani R. 1997. The root form of ferredoxin NADP⁺ oxidoreductase is expressed in rice coleoptiles for the assimilation of nitrate. *Planta* **202,** 397–401.

Neuhaus G, Bowler C, Hiratsuka K, Yamagata H, Chua NH. 1997. Phytochrome-regulated repression of gene expression requires calcium and cGMP. *EMBO Journal* **16,** 2554–2564.

Neuhaus G, Bowler C, Kern R, Chua NH. 1993. Calcium/calmodulin-dependent and –independent phytochrome signal transduction pathways. *Cell* **73,** 937–952.

Newman BJ, Gray JC. 1988. Characterization of a full length cDNA clone for ferredoxin NADP⁺ oxidoreductase. *Plant Molecular Biology* **10,** 511–520.

Nikolaeva MK, Osipova OP. 1982. Light intensity dependent ferredoxin-NADP⁺-reductase activity in higher plants. *Dokladi Akademii Nauk SSSR* **263,** 1513–1516.

Oelmüller R, Bolle C, Tyagi AK, Niekrawietz N, Breit S, Herrman RG. 1993. Characterization of the promoter from the single gene copy encoding FNR from spinach. *Molecular and General Genetics* **237,** 261–272.

Ohyanagi H, Tanaka T, Sakai H, *et al*. 2006. The Rice Annotation Project Database (RAP-DB): hub for *Oryza sativa* ssp. *japonica* genome information. *Nucleic Acids Research* **34,** D741–D744.

Okutani S, Hanke GT, Satomi Y, Takao T, Kurisi G, Suzuki A, Hase T. 2005. Three maize leaf ferredoxin: NADPH oxidoreductases vary in subchloroplast location, expression and interaction with ferredoxin. *Plant Physiology* **139,** 1451–1459.

Onda Y, Matsumara T, Kimata-Ariga Y, Sakakibara H, Sugiyama T, Hase T. 2000. Differential interaction of maize root ferredoxin:NADP⁺ oxidoreductase with photosynthetic and non-photosynthetic ferredoxin isoproteins. *Plant Physiology* **123,** 1037–1045.

Paul MJ, Stitt M. 1993. Effects of nitrogen and phosphorous deficiencies on levels of carbohydrates, respiratory enzymes and metabolites in seedlings of tobacco and their response to exogenous sucrose. *Plant, Cell and Environment* **16,** 1047–1057.

Pschorn R, Rühle W, Wild A. 1988*a*. Structure and function of ferredoxin-NADP⁺-oxidoreductase. *Photosynthesis Research* **17,** 217–229.

Pschorn R, Rühle W, Wild A. 1988*b*. The influence of the proton gradient on the activation of ferredoxin-NADP⁺ oxidoreductase by light. *Zeitschrift fuer Naturforschung Section C Journal of Bioscience* **43,** 207–212.

Quiles MJ, Cuello J. 1998. Association of ferredoxin-NADP oxidoreductase with the chloroplastic pyridine nucleotide dehydrogenase complex in barley leaves. *Plant Physiology* **117,** 235–244.

Ritchie SW, Redinbaugh MG, Shiraishi N, Vrba JM, Campbell WH. 1994. Identification of a maize root transcript expressed in the primary response to nitrate: characterization of a cDNA with homology to ferredoxin NADP⁺ oxidoreductase. *Plant Molecular Biology* **26,** 679–690.

Rühle W, Pschorn R, Wild A. 1987. Regulation of the photosynthetic electron transport during light–dark transitions by activation of the ferredoxin-NADP-oxidoreductase in higher plants. *Photosynthesis Research* **11,** 161–171.

Sakakibara H. 2003. Differential response of genes for ferredoxin and ferredoxin:NADP⁺ oxidoreductase to nitrate and light in maize leaves. *Journal of Plant Physiology* **160,** 65–70.

Schaffner W, Weissmann C. 1973. A rapid, sensitive, and specific method for the determination of protein in dilute solution. *Analytical Biochemistry* **56,** 502–514.

Shin M, Tsujita M, Tomizawa H, Sakihama N, Kamei K, Oshino R. 1990. Proteolytic degradation of ferredoxin NADP reductase during purification from spinach. *Archives of Biochemistry and Biophysics* **279,** 97–103.

Shahak Y, Crowther D, Hind G. 1981. The involvement of ferredoxin-NADP⁺ reductase in cyclic electron transport in chloroplasts. *Biochimica et Biophysica Acta* **636,** 234–243.

Swegle M, Mattoo AK. 1996. Identification and amino acid sequences of tryptic peptides of a novel ferredoxin NADP⁺ oxidoreductase from rice. *Plant Cell Physiology* **37,** 1183–1187.

Takabayashi A, Kishine M, Asada K, Endo T, Sato F. 2005. Differential use of two cyclic electron flows around photosystem I for driving CO_2-concentration mechanism in C_4 photosynthesis. *Proceeding of the National Academy of Sciences, USA* **102,** 16898–16903.

Teicher WC, Scheller HV. 1998. The NAD(P)H dehydrogenase in barley thylakoids is photoactivatable and uses NADPH as well as NADH. *Plant Physiology* **117,** 525–532.

Thompson P, Bowsher CG, Tobin AK. 1998. Heterogeneity of mitochondrial protein biogenesis during primary leaf development in barley. *Plant Physiology* **118,** 1089–1099.

Van Thor JJ, Havaux R, Sjollema M, Joset KA, Hellingwerf KJ, Matthijs HCP. 2000. Salt-inducible photosystem I cyclic electron transfer in *Synechocystis* PCC 6803 relies on binding of ferredoxin-NADP⁺ reductase to the thylakoid membranes via its CpcD phycobilosome-linker homologous N-terminal domain. *Biochimica et Biophysica Acta* **1457,** 129–144.

Van Thor JJ, Hellingwerf KJ, Matthijs HCP. 1998. Characterization and transcriptional regulation of the *Synechocystis* PCC 6803 *petH* gene, encoding ferredoxin-NADP⁺ oxidoreductase: involvement of a novel type of divergent operator. *Plant Molecular Biology* **36,** 353–363.

Wada K, Tsumura M, Aoki K, Morigasaki S, Katoh W, Yamaguchi K, Jin T. 1996. Structure and function of root type ferredoxin NADP⁺ reductase. In: Stevenson KJ, Massey V, Mayhew SG, eds. *Flavins and flavoproteins*. 12, University of Calgary Press. 505–508.

Wang R, Guegler K, LaBrie ST, Crawford NM. 2000. Genomic analysis of a nutrient response in Arabidopsis reveals diverse expression patterns and novel metabolic and potential regulatory genes induced by nitrate. *The Plant Cell* **12,** 1491–1509.

Wang R, Okamoto M, Xing X, Crawford NM. 2003. Microarray analysis of the nitrate response in *Arabidopsis* roots and shoots reveals over 1000 rapidly responding genes and new linkages to glucose, trehalose-6-phosphate, iron and sulfate metabolism. *Plant Physiology* **132,** 556–567.

Wray W, Boulikas T, Wray VP, Hancock R. 1981. Silver staining of proteins in polyacrylamide gels. *Analytical Biochemistry* **118,** 197–203.

Zhang H, Cramer WA. 2004. Purification and crystallization of the cytochrome b6f complex in oxygenic photosynthesis. *Methods in Molecular Biology* **274,** 67–78.